npj | vaccines

Brief communication

Published in partnership with the Sealy Institute for Vaccine Sciences

https://doi.org/10.1038/s41541-025-01308-5

IFN-γ and IL-4 correlate with protection induced by an attenuated malaria vaccine

Tanisha M. Robinson[1], Jessica S. Bolton[1], Elisabeth H. Duncan[1], Elke S. Bergmann-Leitner[1] & Marie Mura[2,3] ✉

Controlled human malaria infections after immunization *via* mosquito bites with radiation attenuated *Plasmodium falciparum* sporozoites are necessary tools to decipher immune signatures of malaria protection. The phenotype of circulating mononuclear innate cells and the PBMC response to in vitro stimulation unraveled correlates of protection from baseline immune response to sporozoite stimulation (IFN-γ secretion and HLA-DR^{high} expression) to vaccine-induced immune factors (IL-4 secretion and CD57^{-} γδ T cell frequency).

Understanding correlates of protection of infectious diseases is key for vaccine development. As malaria sub-unit vaccines (RTS,S/AS01E®, R21/MatrixM®) are implemented in more than 15 African countries, important gaps persist in our understanding of which immune mechanisms mediate sterile protection. Filling these gaps is essential for designing second-generation vaccines with higher efficacy and durable sterile protection. Immunization *via* mosquito bite with radiation attenuated *Plasmodium falciparum* sporozoites (IMRAS) has been considered a "gold standard" malaria vaccine, even though field implementation as a vaccine for larger population may be challenging. Controlled human malaria infection (CHMI) after suboptimal vaccination with IMRAS in a phase I clinical trial (aiming to achieve ~50% vaccine efficacy) enabled profiling of the immune response of protected (P) and non-protected (NP) subjects and establishing immune signatures of protection[1]. By combining immunoprofiling of adaptive responses with an integrative computational approach, we previously associated T cell functionality with protection[2]. Interestingly, the baseline (pre-vaccination) response was already predictive of protection, as reported for other vaccines (e.g., influenza[3]). At the transcriptomic level, PBMC-based RNAseq analysis confirmed differential magnitudes of responses to IMRAS in P vs. NP individuals, with NP subjects not responding to in vitro SPZ stimulation[4]. As the adaptive vaccine immune response is initiated by innate cells, we sought to profile the IMRAS-induced innate immune response and characterize the hypo-responsiveness of NP subjects. We first evaluated the phenotype of circulating mononuclear cells before IMRAS vaccination, after completing the vaccination regimen, and after CHMI (Fig. 1a). Then, we assessed the functionality at each timepoint by measuring cytokine responses of PBMCs or sorted monocytes to specific (SPZ) and non-specific (lipopolysaccharide - LPS) stimulation.

The innate immune signature of IMRAS (Fig. 1) was characterized by a significantly higher frequency of γδ T cells ($p = 0.03$) (Fig. 1b), CD56^{bright} NK cells with a naïve phenotype (CD62L^{+} CD45RO^{-}) ($p = 0.01$) (Fig. 1c), and fewer classical and more intermediate monocytes, although not significant ($p = 0.07$), in response to in vitro SPZ stimulation (Fig. 1d). This response pattern was unchanged after CHMI. Notably, the expression by γδ T cells of CD57 (marker of terminally differentiated cells) was different after IMRAS or CHMI, with a significant increase in CD57^{-} γδ T cells after IMRAS ($p = 0.04$) (Fig. 1e) and a significant increase in CD57^{+} γδ T cells after CHMI (Fig. 1f). The induction of γδ T cells after malaria infection is well known and its importance in protection after attenuated *Pf*SPZ vaccination has been reported[5]. CD57 expression by γδ T cells is associated with chronic exposure to malaria[6] but was not induced by repetitive exposure to irradiated SPZ (IMRAS, five immunization with ~200 mosquito bites/immunization). CD56^{bright} NK cells (Fig. 1c) are a subclass of circulating NK cells with a high potential for migration to secondary lymphoid organs, less cytotoxic activity and a propensity to secrete high levels of cytokines like IFN-γ[7]. Comparing P and NP subjects revealed a significantly higher frequency of HLA-DR^{high} monocytes in response to SPZ stimulation in P subjects ($p = 0.05$), at baseline and after immunization (Fig. 1g, h). This underscores the importance of antigen presentation in this group, in accordance with our previous PBMC-based transcriptomic data[4]. Indeed, this differential expression of HLA-DR was not seen in unstimulated cells, nor in response to LPS. Induction of immunosuppressive monocytes by malaria infection is well known, as well as the increase in NK and γδ T cells[8]. However, we could not statistically associate frequencies of γδ T cells or NK cells subclasses with protection (Fig. 1h).

We then assessed the response of sorted CD14^{+} monocytes to in vitro SPZ stimulation (specific response) or LPS (nonspecific response) by quantifying 10 cytokines (IFN-γ, IL-4, IL-10, IL-12p70, IL-13, IL-1β, IL-2, IL-6, IL-8 and TNF-α) in supernatant after 24 h stimulation (Fig. 2). In response to SPZ stimulation, CD14^{+} monocytes secreted similar levels of

[1]Biologics Research and Development, Walter Reed Army Institute of Research, Silver Spring, MD, USA. [2]Host-Pathogen Interactions, Microbiology and Infectious Diseases Department, Institut de Recherche Biomédicale des Armées, Brétigny-sur-Orge, France. [3]Ecole du Val-de-Grâce, Paris, France. ✉e-mail: marie.mura@intradef.gouv.fr

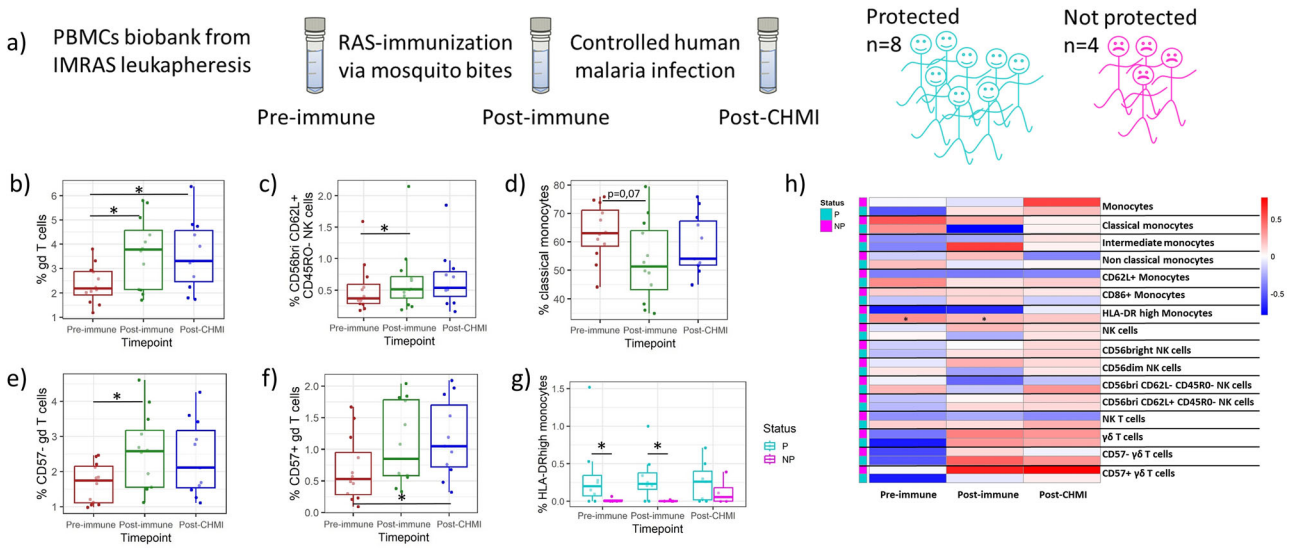

Fig. 1 | Landscape of innate immune cell types responding to in vitro sporozoite stimulation before immunization (pre-immune), after immunization (post-immune) and after CHMI (post-CHMI). a Schematic representation of the biological samples available from the IMRAS clinical trial and the repartition of the protection status after CHMI. Boxplot representing the percentage of **b** γδ T cells, **c** $CD56^{bri}CD62L^{+}CD45RO^{-}$ NK cells, **d** classical monocytes, **e** $CD57^{-}$ γδ T cells and **f** $CD57^{+}$ γδ T cells. **g** Boxplot representing the percentage of HLA-DR^{high} monocytes stratified by protection status (Protected (P) = turquoise, Non-Protected (NP) = magenta). **h** Heatmap visualizes the normalized z-score of the frequencies of innate cells stratified by protection status. The color scale indicates the z-score of the mean cell frequency of P or NP subjects with red color for values above the mean, blue below the mean. Asterisks indicate statistically significant differences: * $p < 0.05$.

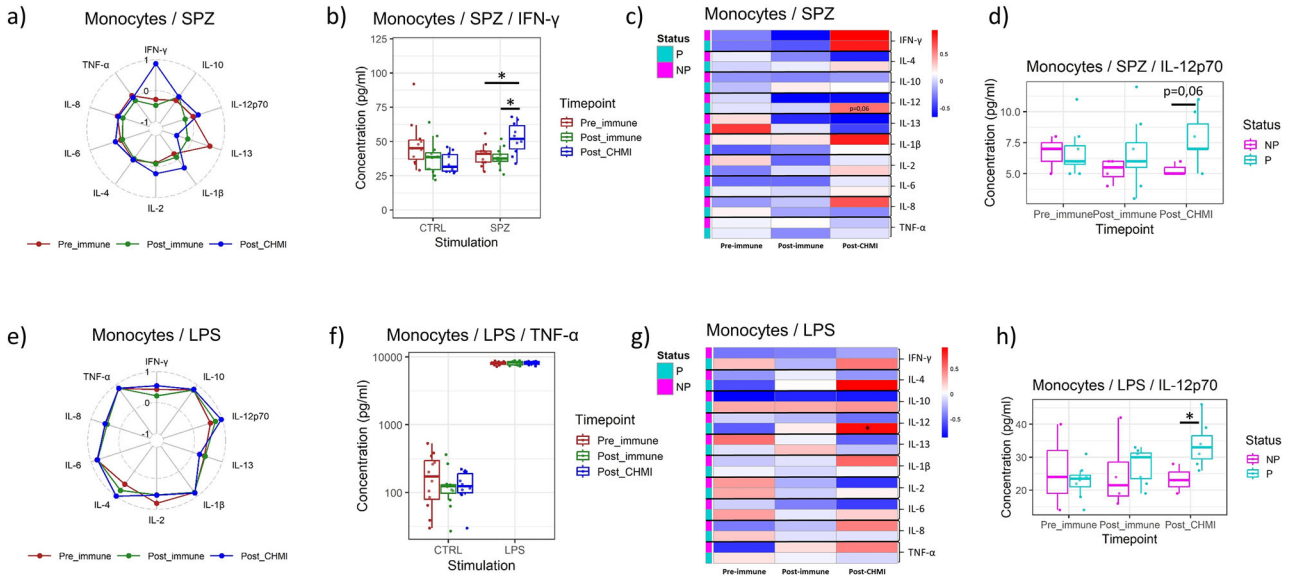

Fig. 2 | Differential cytokine profiles secreted by CD14+ monocytes in response to in vitro specific (SPZ) or nonspecific (LPS) stimulation. a Radar graph representing the normalized z-score of cytokines secreted by monocytes in response to SPZ stimulation before immunization (pre-immune), after immunization (post-immune) and after CHMI (post-CHMI) ($n = 12$). **b** Boxplot representing the concentrations of IFN-γ (pg/ml) in response to SPZ stimulation or left unstimulated (CTRL) at the three time points. **c** Heatmaps visualizing the normalized concentration of cytokines (z-score) in response to SPZ stimulation and stratified by protection status (Protected (P) = turquoise, Non-Protected (NP) = magenta). The color scale indicates the z-score of the mean concentration of P or NP subjects with red color for values above the mean, blue below the mean. (**d**) Boxplot representing the concentration of IL-12p70 (pg/ml) in response to SPZ stimulation at the three time points and stratified by protection status. **e** Radar graph representing the normalized z-score of cytokines secreted by monocytes in response to LPS stimulation at the three time points ($n = 12$). **f** Boxplot representing the concentrations of TNF-α (pg/ml) in response to LPS stimulation or left unstimulated (CTRL) at the three time points. **g** Heatmaps visualizing the normalized concentration of cytokines (z-score) in response to LPS stimulation and stratified by protection status. The color scale indicates the z-score of the mean concentration of P or NP subjects with red color for values above the mean, blue below the mean. **h** Boxplot representing the concentration of IL-12p70 (pg/ml) in response to LPS stimulation at the three time points and stratified by protection status. Asterisks indicate statistically significant differences: *$p < 0.05$.

cytokines before and after immunization (Fig. 2a), but higher levels of IFN-γ after CHMI (Fig. 2a, b). Stratification by protection status revealed that P subjects responded also with increased levels of IL-12p70 ($p = 0.06$) (Fig. 2c, d). The $CD14^{+}$ monocyte response to LPS did not statistically differ at the three time points (Fig. 2e). Notably, TNF-α secretion, a common marker of trained immunity, was similar at baseline, after immunization and CHMI (Fig. 2f). After stratifying by protection status, the cytokine pattern of P subjects was dominated by IFNγ, IL-4, IL-10 and significantly IL-12p70

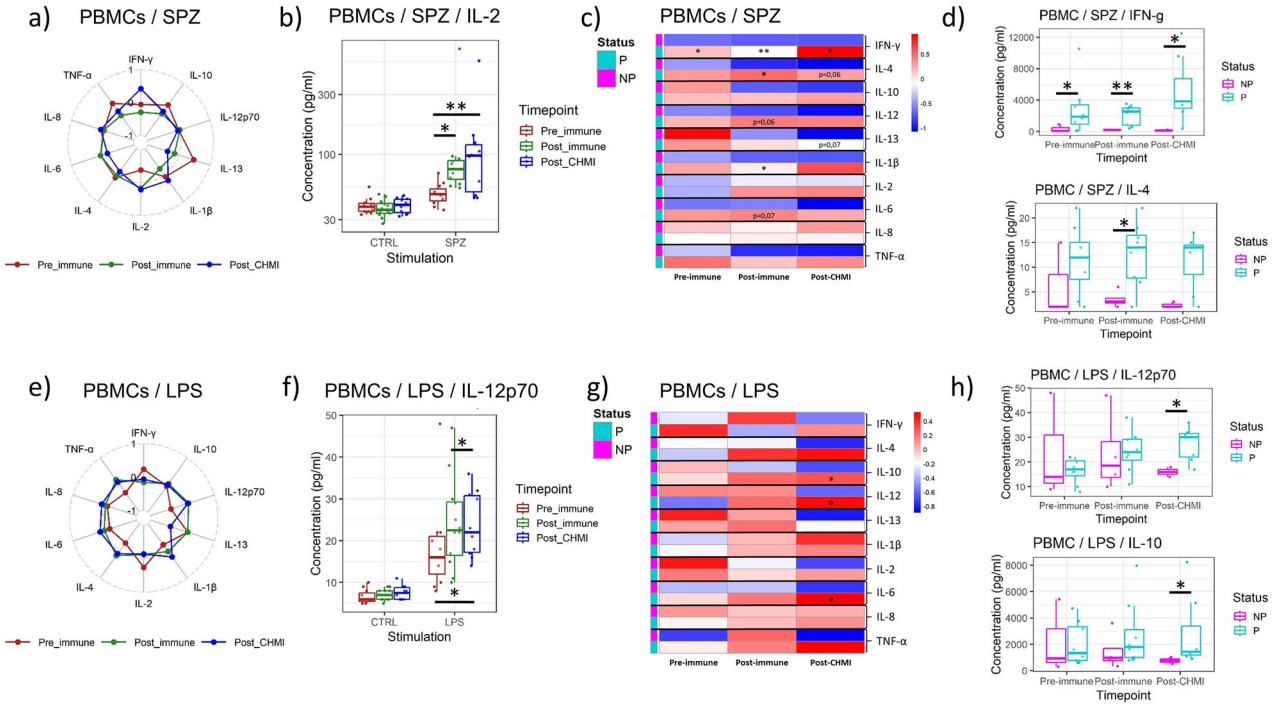

Fig. 3 | Differential cytokine profiles secreted by PBMCs in response to in vitro specific (SPZ) or nonspecific (LPS) stimulation. (**a**) Radar graph representing the normalized z-score of cytokines secreted by PBMCs in response to SPZ stimulation before immunization (pre-immune), after immunization (post-immune) and after CHMI (post-CHMI) ($n = 12$). (**b**) Boxplot representing the concentrations of IL-2 (pg/ml) in response to SPZ stimulation or left unstimulated (CTRL) at the three time points. (**c**) Heatmaps visualizing the normalized concentration of cytokines (z-score) in response to SPZ stimulation and stratified by protection status (Protected (P) = turquoise, Non-Protected (NP) = magenta). The color scale indicates the z-score of the mean concentration of P or NP subjects with red color for values above the mean, blue below the mean. (**d**) Boxplot representing the concentration of IFN-γ and IL-4 (pg/ml) in response to SPZ stimulation at the three time points and stratified by protection status. (**e**) Radar graph representing the normalized z-score of cytokines secreted by PBMCs in response to LPS stimulation at the three time points (n = 12). (**f**) Boxplot representing the concentrations of IL-12p70 (pg/ml) in response to LPS stimulation or left unstimulated (CTRL) at the three time points. (**g**) Heatmaps visualizing the normalized concentration of cytokines (z-score) in response to LPS stimulation and stratified by protection status. The color scale indicates the z-score of the mean concentration of P or NP subjects with red color for values above the mean, blue below the mean. (**h**) Boxplot representing the concentration of IL-12p70 and IL-10 (pg/ml) in response to LPS stimulation at the three time points and stratified by protection status. Asterisks indicate statistically significant differences: $^{*}p < 0.05$ $^{**}p < 0.01$.

($p = 0.02$) whereas NP subjects secreted more pro-inflammatory cytokines, namely TNF-α, IL-8 and IL-1β (Fig. 2g). IL-8 has been shown to have polarizing effects on T cells and regulate their activation[9]. CHMI may have induced in P subjects type-I polarized monocytes producing high levels of IL-12p70 (Fig. 2h). Th1 polarization and IL-12 in malaria protection were previously reported[10].

Establishing the cytokine profile of PBMCs (Fig. 3), IMRAS vaccination induced significantly more IL-2 ($p = 0.01$) in response to SPZ stimulation (Fig. 3a, b). A similar trend was observed after CHMI ($p = 0.01$). The stratification by protection status revealed differential cytokine levels at baseline, especially IFN-γ ($p = 0.04$) (Fig. 3c, d). After completed IMRAS vaccination, PBMCs from NP subjects were hypo-responsive to SPZ, with significantly higher secretion of IFN-γ ($p = 0.004$), IL-4 ($p = 0.04$) and IL-1β ($p = 0.05$) by PBMCs from P subjects (Fig. 3c, d). This profile was maintained after CHMI for IFN-γ (p = 0.02) (Fig. 3c, d). Comparing cytokine profiles of monocytes vs. PBMCs post-CHMI revealed that TNF-α and IL-6 production were higher in PBMCs of P subjects though not statistically significant (Figs. 2c, 3c). IL-6 helps activate T cells, supports their survival, and drives their differentiation toward Th17 and follicular helper T cell (Tfh) subsets while limiting Treg development[11]. TNF-α provides additional costimulatory signals that boost T cell proliferation and promotes Th1 and Th17 responses. Together, these cytokines amplify effector T cell activity while reducing negative feedback.

The PBMC response to LPS confirmed the type-I polarization with higher levels of IL-12p70 secretion after vaccination ($p = 0.04$) and CHMI ($p = 0.01$) (Fig. 3e, f). After CHMI, cytokine profiles of PBMCs significantly changed based on protective status (Fig. 3g): PBMCs from P subjects responded with significantly more IL-12p70 ($p = 0.03$), IL-10 ($p = 0.03$) and IL-6 ($p = 0.03$) (Fig. 3g, h). This suggests that live sporozoites are more potent than attenuated SPZ at training innate cells to acquire nonspecific effector functions. Previous work demonstrated that *Pf*-infected red blood cells and hemozoin can reprogram human adherent PBMCs to hyper-respond to nonspecific stimuli[12] and that CHMI induces lasting changes in monocytes suggestive of trained immunity[13]. Our results suggests that the induced innate training is different depending on the protection status, likely because of large quantities of blood stage parasites in NP subjects.

Finally, we integrated cellular and cytokine data to identify parameters associated with protection using principal component analysis (Fig. 4) and machine learning (random forest model). Discrimination of P and NP subjects was achieved with an accuracy of 86% ($\kappa = 0.58$). The immune measures with the highest relative weights in the prediction were IFN-γ and IL-4 secreting PBMCs in response to SPZ stimulation after IMRAS vaccination, and the frequency of $CD57^{-}$ γδ T cells measured after IMRAS vaccination. IFN-γ secretion, especially at baseline, may involve γδ T cells that are important in shaping the protective $CD8^{+}$ T cell response[14] and/or $CD56^{bright}$ NK cells[7]. In malaria-naïve adults immunized with the radiation-attenuated *Pf*SPZ vaccine or live *Pf*SPZ plus chemoprophylaxis (PfSPZ-cVAC), the γδ T cell frequency and expansion, particularly the Vδ2 subset, was dose dependent and increased IFN-γ expression[15,16]. CD57 expression by γδ T cells was associated with susceptibility to CHMI in our study. In the field, increased expression of CD57 was associated with repeated infections of Ugandan children, and diminished pro-inflammatory cytokine

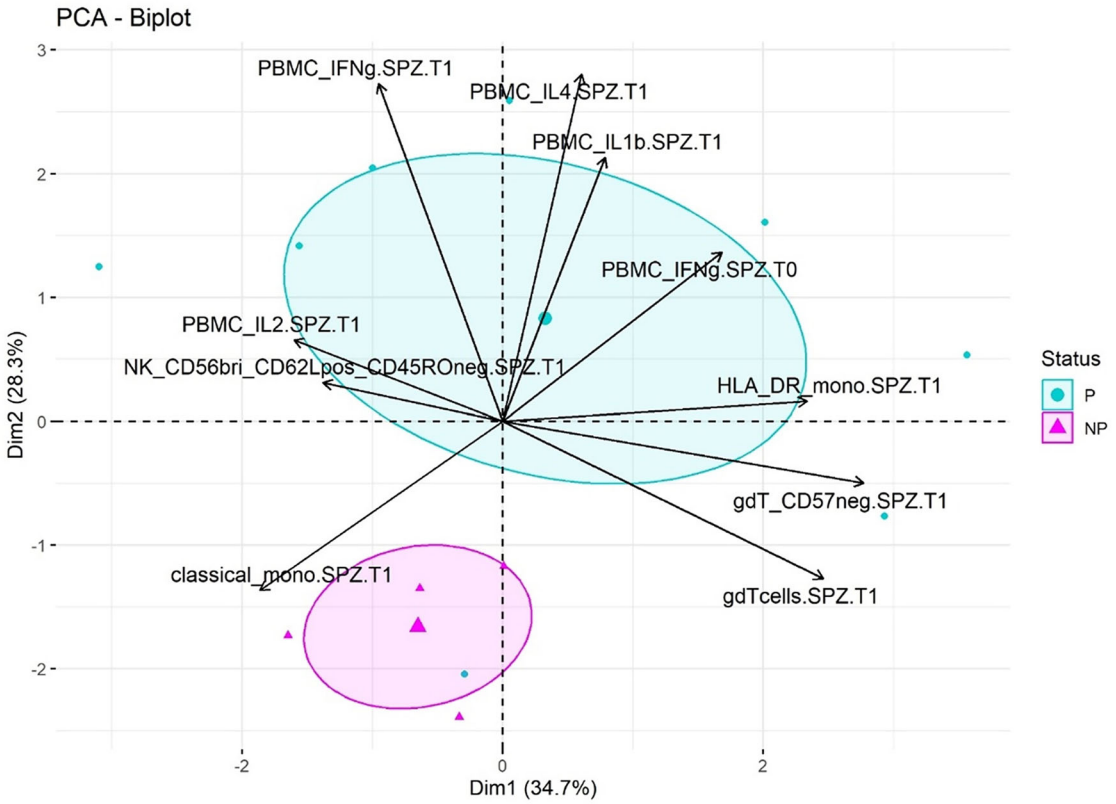

Fig. 4 | Principal component analysis of immune parameters associated with protection. Twelve individuals were plotted on the first (Dim1) and second (Dim2) principal components. The color and shape of the dots indicate the protection status (turquoise = P subjects, magenta = NP subjects). The ellipses represent the 95% confidence interval.

production[6]. IL-4 may have originated from Th2 $CD4^+$ T cells, which were already shown to correlate in vitro with protection in response to antigens from *Pf* erythrocytes[17]. IL-4 is key for developing intrahepatic $CD8^+$ T cell immunity that is critical for malaria protection[18,19].

This study involved a limited numbers of subjects ($n = 12$) but still allowed us to identify critical components of the correlate-of-protection induced by the attenuated sporozoite malaria vaccine. Our results highlight the importance of the innate immune response baseline, mainly (i) IFN-γ secretion in response to in vitro SPZ stimulation presumably from γδ T cells and/or $CD56^{bright}$ NK cell, and (ii) antigen presentation in the form of HLA-DR expression and the frequency of intermediate monocytes. We confirmed at the protein level the previous transcriptomic observation that PBMCs from NP subjects are hypo-responsive to in vitro SPZ stimulation, from baseline to IMRAS and CHMI. Reasons for the hypo-responsiveness are unknown and require further investigation, but others have also reported the importance of baseline immune states to predict vaccine outcomes[3,20]. The current study revealed that the protective immune signature induced by IMRAS vaccination involves adaptive immune responses, specifically IL-4 secretion. We attributed IL-4 secretion to Th2 $CD4^+$ T cells, which may be critical for shaping a protective $CD8^+$ T cell response in the liver. Finally, exposure to live sporozoites significantly modified the cytokine profile of immune cells to non-SPZ stimulus, with type-I polarized monocytes producing high levels of IL-12p70.

Methods

Study design

Human PBMCs were collected under clinical protocol (www.clinicaltrials.gov, trial ID NCT01994525) from an open-label clinical study for identifying biomarkers of protection in two cohorts of healthy malaria-naïve adults[1]. Each volunteer received five immunization sessions involving ~200 bites from infected (*Pf*RAS NF54) *Anopheles stephensi* mosquitoes ($n = 21$). Longitudinal leukapheresis samples (pre-immune, post-immune and post-CHMI timepoints) were available for 8 protected (P) and 4 non-protected (NP) individuals.

PBMCs stimulation and CD14+ monocytes magnetic cell enrichment

Cryopreserved PBMCs from the three timepoints were thawed and $CD14^+$ monocytes were sorted by magnetic enrichment using CD14 positive selection (Miltenyi Biotec, San Diego, CA, USA). Total PBMCs (4×10^5 per well) and sorted $CD14^+$ monocytes (4×10^5 per well) were cultured for 24 h in 96-well plates in media alone (complete RPMI-1640 containing 10% human serum) or stimulated with aseptic, purified, cryopreserved attenuated *Plasmodium falciparum* sporozoites (Sanaria, Rockville, MD, USA) (30,000 SPZ per 4×10^5 cells) or with 10 ng/ml lipopolysaccharide (Invivogen, San Diego, CA, USA).

Flow cytometry

Following cell stimulation, PBCMs were washed and aliquoted for staining with two different surface staining antibody mixtures for 45 minutes at 4 °C. Both included a live/dead fixable dye (Fixable Blue, UV450/50). The innate cell panel included anti-human γδ TCR-PE (clone 11F2), anti-human CD62L-ECD (clone DREG56), anti-human CD56-PE-Cy5.5 (CMSSB), anti-human CD3-PE-Cy7 (clone SK7), anti-human CD38-APC (clone IB6), anti-human CD16-APC-Alexa700 (clone 3G8), anti-human CD8-APC-Alexa750 (clone 3B5), anti-human CD4-Krome orange (clone 13B8.2), anti-human CD57-Pacific blue (clone NC1), anti-human CD45RA-BV785 (clone HI100), anti-human CD45RO-BUV737 (clone UCHL1), anti-human TCR Va24-ja18-FITC (clone 6B11). The monocyte panel included anti-human CD14-Viogreen (clone REA599), anti-human

CD16-APC-Alexa700 (clone 3G8), anti-human CD3-Vioblue (clone BW264/56), anti-human CD19-PercpVio700 (clone LT19), anti-human CD56-PE-Cy5.5 (clone CMSSB), anti-human CD36-BV650 (clone CLB-IVC7), anti-human CD62L-ECD (clone DREG56), anti-human HLA-DR-PE (clone REA805), anti-human CD86-PE-Vio770 (clone REA968), anti-human CD11c-FITC (clone REA618), anti-human CCR2-APC (clone REA264). Cells were washed in FACS solution and acquired on a BD LSR Fortessa. Cell viability of thawed PBMCs was > 92% as measured on a Luna-FL™ Dual fluorescence cell counter. Flow cytometric data were analyzed using FlowJo V10. For both panels, cells were first gated based on Forward- (FSC) *vs* Sideward scatter (SSC), then single cells, followed by viability and lineage markers. NK cells were defined as $CD3^-$ and $CD56^+$ cells, and then divided into CD56 bright/dim expression, and CD62L/CD45R0 expression. NK T cells were defined as $CD3^+$ $CD56^+$ γδ TCR^-, and invariant NK T cells (iNK T cells) were defined as NK T cells expressing the TCR Va24-ja18. γδ T cells were defined as $CD3^+$ and γδ TCR^+, and then divided into $CD57^+$ and $CD57^-$ population. Monocytes were divided into classical, intermediate, and non-classical monocytes based on CD14 and CD16 expression. Expression of CD62L, HLA-DR and CD86 was assessed for each monocyte subpopulation.

Electrochemiluminescence assay

Secretion of ten cytokines (IFN-γ, IL-4, IL-10, IL-12p70, IL-13, IL-1β, IL-2, IL-6, IL-8 and TNF-α) was assessed in the cell culture supernatant using the V-PLEX human pro-inflammatory panel 1 (Meso Scale Discovery® (MSD), catalog number K15049D). Briefly, plates were washed 3-times, 150 µl/well with 1X wash buffer. Culture supernatant samples were diluted 2-fold using Diluent 2, and 50 µl/well (V-PLEX human pro-inflammatory panel 1 plate) were added. Samples were run as singlets. Standards were prepared according to the MSD instructions, diluted 4-fold using Diluent 2, and 50 µl was added to each well. The standard curve samples were set up in duplicate. After incubation on a shaker at 4 °C overnight for 16 h, the plate was washed 3-times and 25 µl of the diluted detection antibodies directed against the 10 selected cytokines were added for another 2 h of incubation on a plate shaker at room temperature. Finally, the addition of 150 µl of 2X read buffer T after three washing steps allowed the detection of a specific chemiluminescent signal with the MESO QuickPlex SQ 120, per manufacturer's instructions. The data generated were analyzed with the Discovery Workbench software version 4. Each cytokine concentration was expressed in pg/ml (means and standard deviations in supplementary tables 1-4).

Statistical analysis

Statistical analysis was performed using R (version 4.0.5) and R Studio (version 2025.1.3.1093) software. The longitudinal analysis over the time was done using the non-parametric Kruskal-Wallis test, then the Dunn post-hoc test. The comparison of the protection status was done using the non-parametric Wilcoxon-Mann-Whitney test. A $p < 0.05$ was considered significant. The random forest model (based on the R caret package) was trained using the repeated *cv* method, subsampling the data set by 5-fold and resampling 100 times. The *varImp* function was used to determine the variable importance for each generated model, and the average variable importance across all models was reported to assess the relative importance of each factor at predicting the protection status. The accuracy of the model was the percentage of correctly classified individuals. The κ value was normalized at the baseline of random chance on the dataset and was of particular interest for an imbalanced model, as is the case in the study.

Data availability

The data are contained within the manuscript. Analysis scripts in R can be made available upon request from the corresponding author.

Received: 30 July 2025; Accepted: 3 November 2025;
Published online: 24 December 2025

References

1. Hickey, B. et al. IMRAS-A clinical trial of mosquito-bite immunization with live, radiation-attenuated P. falciparum sporozoites: impact of immunization parameters on protective efficacy and generation of a repository of immunologic reagents. *PLoS ONE* **15**, e0233840 (2020).
2. Mura, M. et al. Immunoprofiling identifies functional B and T cell subsets induced by an attenuated whole parasite malaria vaccine as correlates of sterile immunity. *Vaccines* **10** https://doi.org/10.3390/vaccines10010124 (2022).
3. Tsang, J. S. et al. Improving vaccine-induced immunity: can baseline predict outcome?. *Trends Immunol.* **41**, 457–465 (2020).
4. Mura, M. et al. Human transcriptional signature of protection after Plasmodium falciparum immunization and infectious challenge via mosquito bites. *Hum. Vaccin Immunother.* **19**, 2282693 (2023).
5. Dantzler, K. W. & Jagannathan, P. gammadelta T cells in antimalarial immunity: new insights into their diverse functions in protection and tolerance. *Front. Immunol.* **9**, 2445 (2018).
6. Jagannathan, P. et al. Loss and dysfunction of Vdelta2(+) gammadelta T cells are associated with clinical tolerance to malaria. *Sci. Transl. Med.* **6**, 251ra117 (2014).
7. Poli, A. et al. CD56bright natural killer (NK) cells: an important NK cell subset. *Immunology* **126**, 458–465 (2009).
8. Dooley, N. L. et al. Single cell transcriptomics shows that malaria promotes unique regulatory responses across multiple immune cell subsets. *Nat. Commun.* **14**, 7387 (2023).
9. Meniailo, M. E. et al. Direct effects of interleukin-8 on growth and functional activity of T lymphocytes. *Int. Immunopharmacol.* **50**, 178–185 (2017).
10. Luty, A. J. et al. Low interleukin-12 activity in severe Plasmodium falciparum malaria. *Infect. Immun.* **68**, 3909–3915 (2000).
11. Grebenciucova, E. & VanHaerents, S. Interleukin 6: at the interface of human health and disease. *Front. Immunol.* **14**, 1255533 (2023).
12. Schrum, J. E. et al. Cutting edge: plasmodium falciparum induces trained innate immunity. *J. Immunol.* **200**, 1243–1248 (2018).
13. Walk, J. et al. Controlled human malaria infection induces long-term functional changes in monocytes. *Front. Mol. Biosci.* **7**, 604553 (2020).
14. Zaidi, I. et al. gammadelta T cells are required for the induction of sterile immunity during irradiated sporozoite vaccinations. *J. Immunol.* **199**, 3781–3788 (2017).
15. Mordmuller, B. et al. Sterile protection against human malaria by chemoattenuated PfSPZ vaccine. *Nature* **542**, 445–449 (2017).
16. Seder, R. A. et al. Protection against malaria by intravenous immunization with a nonreplicating sporozoite vaccine. *Science* **341**, 1359–1365 (2013).
17. Bergmann, E. S., Ballou, R. W. & Krzych, U. Detection of CD4+CD45RO+ T lymphocytes producing IL-4 in response to antigens on Plasmodium falciparum erythrocytes: an in vitro correlate of protective immunity induced with attenuated Plasmodium falciparum sporozoites. *Cell Immunol.* **180**, 143–152 (1997).
18. Morrot, A. & Rodrigues, M. M. Tissue signatures influence the activation of intrahepatic CD8(+) T cells against malaria sporozoites. *Front. Microbiol.* **5**, 440 (2014).
19. Carvalho, L. H. et al. IL-4-secreting CD4+ T cells are crucial to the development of CD8+ T-cell responses against malaria liver stages. *Nat. Med.* **8**, 166–170 (2002).
20. Nehar-Belaid, D. et al. Baseline immune states (BIS) associated with vaccine responsiveness and factors that shape the BIS. *Semin. Immunol.* **70**, 101842 (2023).

Acknowledgements

We thank Judith Epstein, the Naval Medical Research Center (NMRC) Clinical Trials Center, and the Malaria Department Clinical Immunology Laboratory staff that conducted the clinical trial and processed/cryopreserved clinical samples, respectively. This work was supported by the Military Infectious

Disease Research Program. Material has been reviewed by the Walter Reed Army Institute of Research. There is no objection to its presentation and/or publication. The opinions or assertions contained herein are the private views of the authors, and are not to be construed as official, or as reflecting the views of the Department of the Army or the Department of Defense. The investigators have adhered to the policies for protection of human subjects as prescribed in AR 70-25. This paper has been approved for public release with unlimited distribution. E.S.B.-L. and E.H.D. are government employees. Title 17 U.S.C. § 105 provides that "Copyright protection under this title is not available for any work of the United States Government, but the United States Government". Title 17 U.S.C. § 101 defines US Government work as "work prepared by a military service member or employee of the US Government as part of that person's official duties.

Author contributions

Conceptualization, M.M. and E.S.B.-L.; methodology, M.M, T.M.R., J.S.B., and E.H.D.; software, M.M.; formal analysis, M.M.; resources, E.S.B.-L.; writing, M.M.; visualization, M.M..; supervision, M.M. and E.S.B.-L.; All authors have read, edited, and agreed to the published version of the manuscript.

Competing interests

The authors declare no competing interests.

Additional information

Supplementary information The online version contains supplementary material available at https://doi.org/10.1038/s41541-025-01308-5.

Correspondence and requests for materials should be addressed to Marie Mura.